

---

This is an electronic reprint of the original article.  
This reprint may differ from the original in pagination and typographic detail.

Arkkio, A.; Cederstrom, S.; Awan, H. Asad Ali; Saarakkala, S. E.; Holopainen, T. P.

## Additional Losses of Electrical Machines under Torsional Vibration

*Published in:*  
IEEE Transactions on Energy Conversion

*DOI:*  
[10.1109/TEC.2017.2733546](https://doi.org/10.1109/TEC.2017.2733546)

Published: 01/01/2018

*Document Version*  
Peer-reviewed accepted author manuscript, also known as Final accepted manuscript or Post-print

*Please cite the original version:*  
Arkkio, A., Cederstrom, S., Awan, H. A. A., Saarakkala, S. E., & Holopainen, T. P. (2018). Additional Losses of Electrical Machines under Torsional Vibration. *IEEE Transactions on Energy Conversion*, 33(1), 245-251.  
<https://doi.org/10.1109/TEC.2017.2733546>

---

This material is protected by copyright and other intellectual property rights, and duplication or sale of all or part of any of the repository collections is not permitted, except that material may be duplicated by you for your research use or educational purposes in electronic or print form. You must obtain permission for any other use. Electronic or print copies may not be offered, whether for sale or otherwise to anyone who is not an authorised user.

# Additional Losses of Electrical Machines under Torsional Vibration

A. Arkkio, S. Cederström, H. Asad Ali Awan, S. E. Saarakkala and T. P. Holopainen

**Abstract**—Electric drive trains have a torsional rigid-body vibration mode at a small, non-zero frequency. If an excitation occurs close to this frequency, the vibration amplitude may grow large and the electrical machine may suffer from significant additional losses. Standards set constraints on the oscillating torque in the shaft coupling and on the harmonics of line current. They indirectly limit the vibration amplitude and losses of the machines.

Time-discretized finite-element analysis was used to study the losses of six induction and six synchronous machines under torsional vibration restricted by the constraints above. All the machines were supplied from sinusoidal voltage sources. In the worst cases of the induction motors, the vibration increased the electromagnetic total loss by about 20%. The constraints on synchronous machines are milder than those for induction machines. In this case, the maximum increase of the loss was 75%. The limit on the harmonic currents is essential from the loss point of view. Without this limit, the additional loss at the rigid-body resonance would lead to a temperature rise high enough to destroy the insulation system of the machine.

The method of loss analysis was validated by measured results.

**Index Terms**—additional losses, electrical machines, finite element analysis, temperature rise, torsional vibration

## I. INTRODUCTION

TORSIONAL vibrations occur in every drive train. If a simple drive train consists of an electrical motor, shaft coupling and a load machine, the system has two basic torsional vibration modes, the rigid-body mode and the first elastic mode.

In purely mechanical drive trains, the rigid-body mode occurs at zero frequency. When an electrical machine is present, the interaction of the stator and rotor magnetic fields forms a torsional spring effect that together with the inertia of the whole drive train lead to a vibration mode at a small non-zero natural frequency. The same attribute, rigid-body, will be used here for the lowest mode of the electromechanical system

as is commonly used for the lowest mode of the purely mechanical rotor system. There is no significant twisting in the rigid-body mode. In spite of this, the rotational oscillation of the rigid-body mode will be called torsional vibration.

The natural frequency of the rigid-body mode is typically some Hertz for larger machines and some tens of Hertz for smaller ones. As the torsional twisting is small, the mechanical damping of the rigid-body mode is negligible, and the vibration amplitude may grow large, even to a significant part of the pole pitch of the electrical machine.

In the second mode of our simple drive train, the first elastic mode, the torsional twisting mainly occurs across the shaft coupling. Its natural frequency depends on the stiffness of the shaft coupling together with the inertias of the motor and load but it is typically larger than the natural frequency of the rigid-body mode. The construction of the shaft coupling often limits the vibration amplitude to a relatively small value. A small-amplitude of vibration means that the electromagnetic losses associated with the vibration also remain small. In this paper, we shall focus on relatively small vibration frequencies and relatively large vibration amplitudes, i.e. we are mainly interested in the rigid-body mode of vibration.

A reciprocating compressor run by an electrical motor is the basic example of drive trains with large torsional excitations. Part of the excitations occur at low frequencies close to the rigid-body natural frequency. Another case is a diesel generator with ignition problems. If one of the cylinders does not work properly, torque pulsation occurs at a relatively low frequency. For an 18-cylinder four-stroke engine running an eight-pole 50 Hz generator, the excitation frequency would be 6.25 Hz, which is close to the rigid-body natural frequency of the drive train.

Many papers have been written on modelling and measuring the torsional vibrations of electric drive trains [1-5], particularly, for turbine generator sets [6-8]. Damping of torsional vibration of a wind generator was studied in [9]. Yet, no papers could be found that would focus on the losses of electrical machines under torsional vibration.

This paper studies the losses caused by torsional oscillations in electrical machines. As numerical models will be used, it would be convenient to constraint the study just on the essential part of the frequency - amplitude plane of torsional vibration. We could not find a standard that would directly limit the torsional vibration amplitude of a drive train. However, there are standards that put constraints on the torque of the shaft coupling and on the harmonic stator currents. As

The manuscript was first submitted for review 2016-12-22.

This research was supported by the European Research Council (ERC) within the European Union's Seventh Framework Programme (FP7/2007-2013)/ERC under Grant 339380 and by the Finnish Cultural Foundation Grant 00132280.

A. Arkkio, S. Cederström, H. Asad Ali Awan and S. E. Saarakkala are with Aalto University, School of Electrical Engineering, Finland (e-mails: antero.arkkio@aalto.fi, samuli.cederstrom@aalto.fi, hafiz.awan@aalto.fi, seppo.saarakkala@aalto.fi).

T.P. Holopainen is with ABB Oy, Helsinki, Finland (e-mail: timo.holopainen@fi.abb.com).

these quantities are proportional to the amplitude of the torsional oscillation, they can be used for constraining the frequency and amplitude range of the torsional oscillation of the study.

API Standard 671 [10] specifies that a shaft coupling should as a minimum stand torque loadings that are 1.5 times larger than the steady-state rated torque. This can be interpreted that a shaft coupling should stand the rated torque plus a vibrating torque with an amplitude of half the rated torque.

ANSI/API Standard 618 [11] states that in synchronous motor - compressor installations the current variations should be restricted to less than 66% of the full load current. For induction motors, this percentage is 40%. As torsional vibration induces two harmonic components in the stator current, we interpret the conditions above that the harmonic distortion of the stator current at rated load should not exceed 66% for synchronous machines or 40% for induction machines.

## II. METHODS OF ANALYSIS

### A. Finite element analysis and the losses

Two-dimensional finite-element models were used. End-winding impedances of the stator and rotor windings were added to the circuit equations to approximately model the 3D end-winding fields. The trapezoidal rule was used for time-discretization. The field and circuit equations were discretized and solved together [12]. Moving-band technique in the air gap of the machine was used for rotating the rotor [13]. The torque was computed using Coulomb's method [14].

The currents and resistive losses of the windings were obtained when solving the combined field and circuit equations using FEM. The eddy-current losses in the laminated stator and rotor cores were also included in the FEA using the simple method presented by Knight et al. [15]. The hysteresis losses of the core were estimated in post-processing [16].

### B. Constraints on vibration amplitude

It is assumed that the shaft coupling of the electrical machine can continuously transmit an oscillating torque of amplitude equal to half of the rated torque of the electrical machine. Assuming that the mechanical damping is negligible the equation of motion for the rotor of the electrical machine is

$$J \frac{d^2 \Theta}{dt^2} + C_{em} \frac{d\Theta}{dt} + K_{em} \Theta = T \quad (1)$$

where  $J$  is the mass of inertia of the rotor,  $C_{em}$  is the coefficient of electromagnetic viscous damping,  $K_{em}$  is the stiffness coefficient associated with the magnetic field and  $T$  is the external torque acting on the rotor. The electromagnetic damping and stiffness coefficients for an electrical machine can be obtained from time-discretized finite element analysis as described in [17].

Assuming harmonic oscillations, we can use phasor variables for solving the equation of motion. Using trial functions

$$\Theta = \text{Re}(\hat{\Theta} e^{j\omega t}); \quad T = \text{Re}(\hat{T} e^{j\omega t}) \quad (2)$$

for the angular displacement and for the external torque, we get a relation between the phasors of the angular displacement and external torque

$$\hat{\Theta} = \frac{(K_{em} - J\omega^2) - j\omega C_{em}}{(K_{em} - J\omega^2)^2 + \omega^2 C_{em}^2} \hat{T} \quad (3)$$

As discussed related to the API standard 671, we fix the amplitude of the oscillating torque to half of the rated torque in Eq. (3). In this way, we obtain a curve limiting the vibration amplitude as a function of frequency. The limiting curve is shown in red color in Figure 1 (Torque limit). It was computed for a 12 MW synchronous motor.

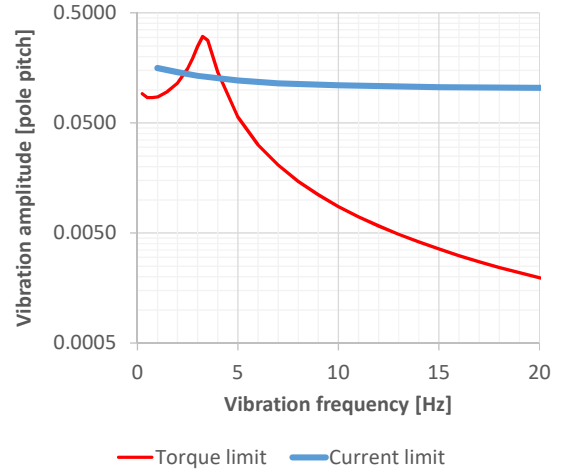


Fig. 1. Limiting curves for the vibration amplitude of a 12 MW synchronous motor. The allowed vibration region is below these curves.

The harmonic distortion of the stator current puts another limit for the vibration amplitude, as stated in API Standard 618. This curve is shown in blue color (Current limit) in Figure 1. It was obtained as described below.

Torsional vibration induces harmonic stator currents at two frequencies

$$f = f_s \pm f_v \quad (4)$$

where  $f_s$  is the supply frequency and  $f_v$  the torsional vibration frequency.

Figure 2 shows the relative amplitudes of these two currents computed for a 12 MW six-pole synchronous motor as functions of vibration amplitude. The vibration frequency is 7 Hz which induces the 43 Hz and 57 Hz harmonic components in the stator current. The percentage of harmonic distortion of the stator current is defined

$$D_h = \frac{100}{i_1} \sqrt{\sum_n i_n^2} \quad (5)$$

where  $i_1$  is the fundamental harmonic of the stator current at

the rated load and index  $n$  runs over the two harmonics at frequencies  $f_s \pm f_v$  (Eq. 4), only. Using the currents of Figure 2, the 66% distortion limit is reached at the vibration amplitude of 0.115 pole pitches.

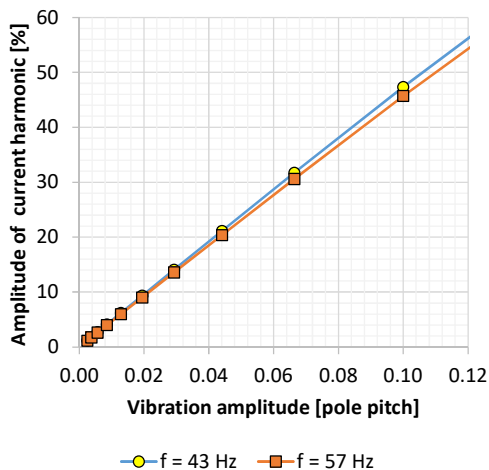


Fig. 2. Relative amplitudes of vibration harmonics in the stator current of a 12 MW synchronous motor. The vibration frequency is 7 Hz and the motor is operated at the rated power. The currents are scaled by the rated current of the machine.

Figure 1 shows the limiting curves for the amplitude of torsional vibration of the 12 MW motor. The constraint from the torque of the shaft coupling (Eq. 3) allows significant vibration amplitudes only at low frequencies. At frequencies smaller than 10 Hz the amplitude can be large enough to produce significant additional losses. The constraint on current distortion is active just around the electromechanical resonance frequency for the synchronous machine. This constraint is stricter for induction motors and cuts most of the resonance peaks away from their allowed region of vibration.

The region of interest depends on the size of the machine. For a 37 kW four-pole cage induction motor, the resonance peak occurs at about 18 Hz, and from the loss point of view, the vibrations are large enough up to about 40 Hz.

### III. RESULTS

#### A. Computed results

Twelve electrical machines were analyzed. Six of them are cage induction motors, and six synchronous machines. They are briefly introduced in Table I.

All the induction machines are cage induction motors. The synchronous machine SM1 is a permanent magnet assisted synchronous reluctance motor. SM2 is a permanent magnet motor with embedded magnets and damper bars on the pole shoe. SM3 – SM6 are conventional salient pole machines with field and damper windings.

The 12 machines of Table I were studied under torsional vibration using the time-discretized FEA model described in Section II A. All the machines were supplied from sinusoidal voltage sources. The interesting ranges of the vibration frequency and amplitude were first defined by computing the amplitude limiting curves like the ones in Figure 2 for all the

machines.

TABLE I  
MACHINES STUDIED  
(The powers are given in kW, the dimensions in mm)

Induction machines	IM1	IM2	IM3	IM4	IM5	IM6
Used as	motor	motor	motor	motor	motor	motor
Rated power	18	30	37	3500	3725	4500
Number of poles	6	2	4	4	8	2
Air-gap diameter	235	190	200	710	720	620
Core length	180	185	250	920	1090	800

Synchronous machines	SM1	SM2	SM3	SM4	SM5	SM6
Used as	motor	motor	motor	gener.	motor	gener.
Rated power	40	45	6000	8150	12000	14000
Number of poles	4	4	20	8	6	14
Air-gap diameter	200	200	2120	1150	1340	2020
Core length	250	250	850	1150	1150	950

The limiting curves together with the loss results for machines IM1, IM3, IM5, SM2, SM4 and SM6 are shown in Figures 3 – 8. The percentage increase of the total electromagnetic loss caused by torsional vibration is shown on the frequency - amplitude plane as equivalent lines. The two thicker lines in the figures present the curves limiting the vibration amplitude. They were obtained by setting the oscillating torque at the shaft to half of the rated torque of the machine (red dashed line) and the harmonic distortion of stator currents to 40% for the induction machines and 66% for the synchronous machines (blue dotted line). The dc component of the shaft torque was equal to the rated torque of the machine in all the cases.

The constraint on vibration amplitude from the current distortion has a local maximum at the supply frequency of the machine, for instance, at 50 Hz in Figure 6. The losses on the other hand, have a local minimum at this frequency. The source for both these phenomena is the  $f_s - f_v$  harmonic current that vanishes at the supply frequency.

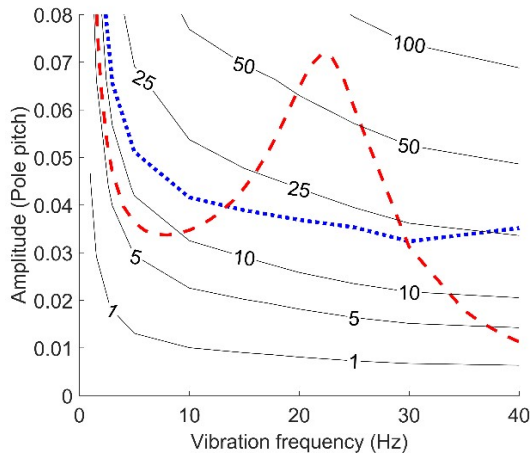


Fig. 3. Additional electromagnetic loss caused by torsional vibration in the 18 kW six-pole cage induction motor IM1. The losses are given in percentage of the rated-load loss without vibration.

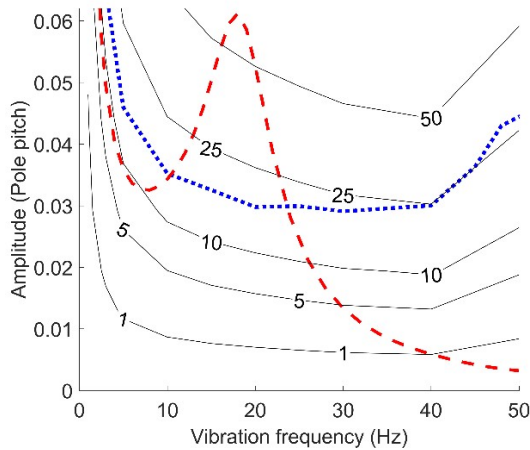


Fig. 4. Additional electromagnetic loss caused by torsional vibration in the 37 kW four-pole cage induction motor IM3. The losses are given in percentage of the rated-load loss without vibration.

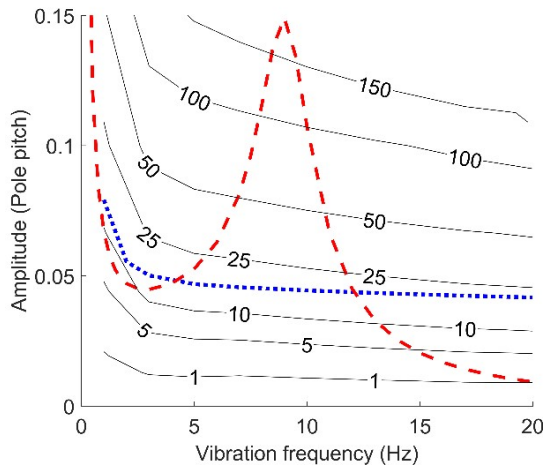


Fig. 5. Additional electromagnetic loss caused by torsional vibration in the 3.7 MW eight-pole cage induction motor IM5. The losses are given in percentage of the rated-load loss without vibration.

By studying the constraint lines in the figures, one can see that the constraint on the harmonic distortion of stator current effectively cuts away the vibration region of rigid-body resonance from induction motors. This constraint is milder for synchronous machines and only the tips of the resonance

peaks are cut away from their allowed region of vibration.

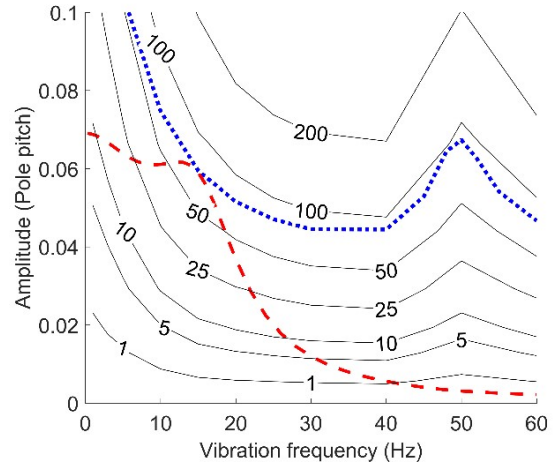


Fig. 6. Additional electromagnetic loss caused by torsional vibration in the 45 kW four-pole permanent-magnet motor SM2. The losses are given in percentage of the rated-load loss without vibration.

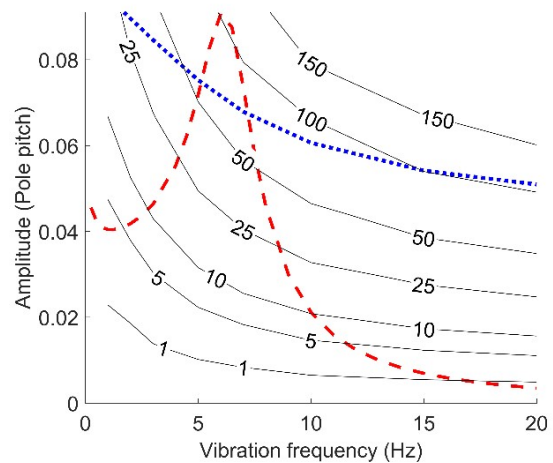


Fig. 7. Additional electromagnetic loss caused by torsional vibration in the 8 MVA eight-pole synchronous generator SM4. The losses are given in percentage of the rated-load loss without vibration.

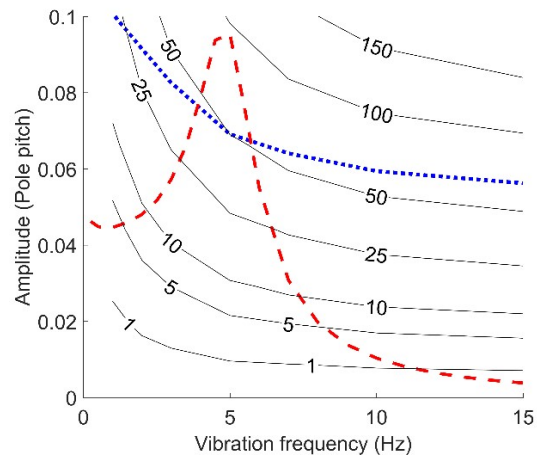


Fig. 8. Additional electromagnetic loss caused by torsional vibration in the 14 MVA fourteen-pole synchronous generator SM6. The losses are given in percentage of the rated-load loss without vibration.

The dashed and dotted limiting curves in Figures 3-8 typically have two intersection points. The maximum

additional loss seems to occur at the higher-frequency intersection point. By picking up the values of the additional loss from these points in Figures 3-8, we come to the conclusion that torsional vibration may increase the losses of synchronous machines up to 75% and those of induction machines up to 20%. The results obtained for the six other machines in Table I agree with these percentages.

The effect of loading on the additional losses can be seen by comparing Figures 9a and 9b computed for the 6 MW synchronous motor SM3. When computing the results of Figure 9a, the average torque was zero. The results in Figure 9b are for the full load operation. In both the cases, the additional losses are scaled by the rated electromagnetic loss of the machine. Figure 9 implies that the loading has just a minor effect on the additional loss.

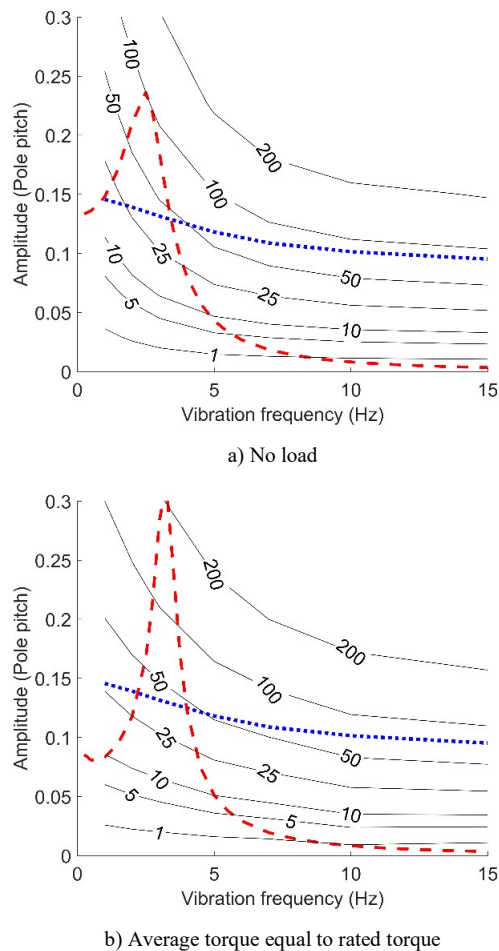


Fig. 9. Effect of loading on the additional loss. The 6 MW synchronous motor (SM3) has been simulated at no load (a) and at the rated load (b).

### B. Validation measurements

The loss model used for the machines in torsional vibration was validated by studying the 37 kW cage induction motor (IM3). Figure 10 shows the measuring set-up. The machine under test is coupled to a 45 kW cage induction machine with a torque transducer. The test machine is supplied from the grid, the 45 kW exciter machine from a frequency converter. Through a proper control of the frequency converter the exciter machine produces a shaft torque that includes both a dc

component and an oscillating component.

The frequency converter controls the air-gap torque of the exciter machine. In this section, the controlled air-gap torque of the exciter machine is called for brevity the excitation torque. Because of the inertia of the exciter machine, the excitation torque is not the same as the shaft torque.

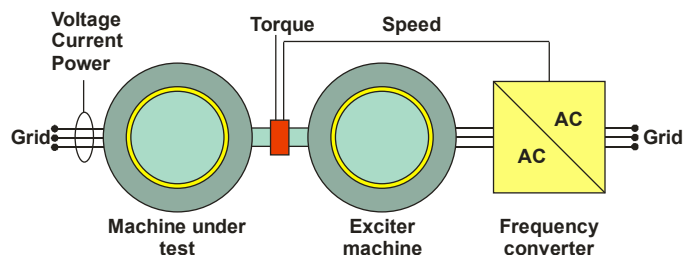


Fig. 10. Measuring set-up.

The available frequency converter could only supply power from the grid to the machines, not the other way around. Thus, we had to operate the test machine as a generator feeding power to the grid. The one directional power flow also limited the oscillating torque component to be smaller than the dc component.

As there are several frequencies involved in a machine under torsional vibration, the power measurement became somewhat challenging. The power analyzer selected its integration period based on the fundamental frequency of the supply voltage. As the frequency of torsional vibration was independent from this, there was relatively large variation between the measured samples of input power. The worst cases occurred when the full measuring period, which included the times needed for the sampling, calculation and data transfer, was close to the period of the vibration frequency. In this case, a spurious “low-frequency” periodicity appeared in the measured data. We tried to extract the proper average power from the measured data by taking this periodicity into account and averaging over 50-80 measured samples.

Figure 11 shows a comparison of the measured and computed electromagnetic losses. The average value of the excitation torque was 125 Nm and its oscillating component 120 Nm. The oscillation frequency was varied from 2 to 20 Hz. It should be kept in mind that this excitation torque acted on the rotor of the exciter machine, not on the rotor of the test machine. In the simulations, the equations of motion of the drive train were solved together with magnetic field of the test machine [18]. The input torque in the simulation was as described above for the measurements.

The measured and computed total electromagnetic losses agree well in Figure 11a. Somewhat bigger relative differences are found in the additional losses of Figure 11b. A larger vibration amplitude would have improved the accuracy of loss segregation but the available torsional excitation system did not allow this. All in all, the measured and computed results agree well enough to build confidence in the methods used for the vibration and loss study.

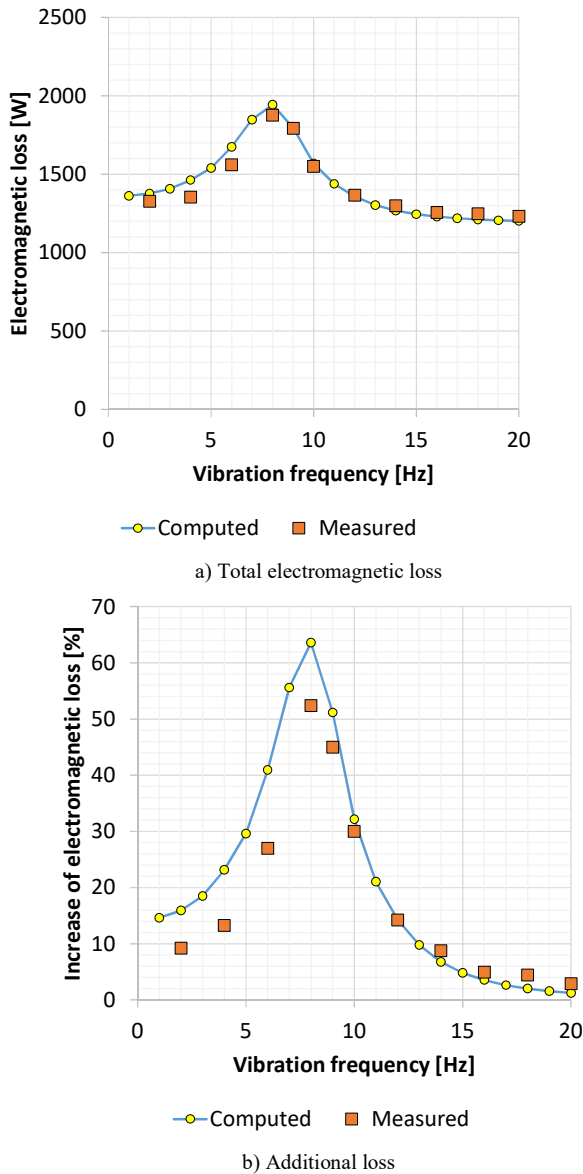


Fig. 11. Measured and computed electromagnetic losses of the 37 kW cage induction motor under torsional excitation.

#### IV. DISCUSSION

According to the simulation results of the 37 kW motor, roughly one third of the additional loss came from the resistive loss of the stator winding and two thirds from the resistive loss of the rotor cage. The core loss was almost independent from the vibration. The results of the other 11 machines follow similar lines. The main part of the additional loss always came from the rotor cage. The larger the machine, the larger was the share of the resistive rotor loss. In all the studied cases, the additional oscillating component in the rotation speed increased the core losses only slightly from the case of constant speed. Core losses can be safely dropped out from analysis if only the main effects of vibration on the losses are studied.

To clearly show the effect of torsional vibration on the stator current, the 6 MW synchronous motor (SM3) was simulated for two cases of loading. In the first one, the load

torque was constant, equal to the rated torque of the motor. In the second case, the load torque had both the constant and oscillating parts. The constant part was equal to the rated torque and the oscillating part was half of the rated torque. The oscillation frequency was 4 Hz. The results are shown in Figure 12.

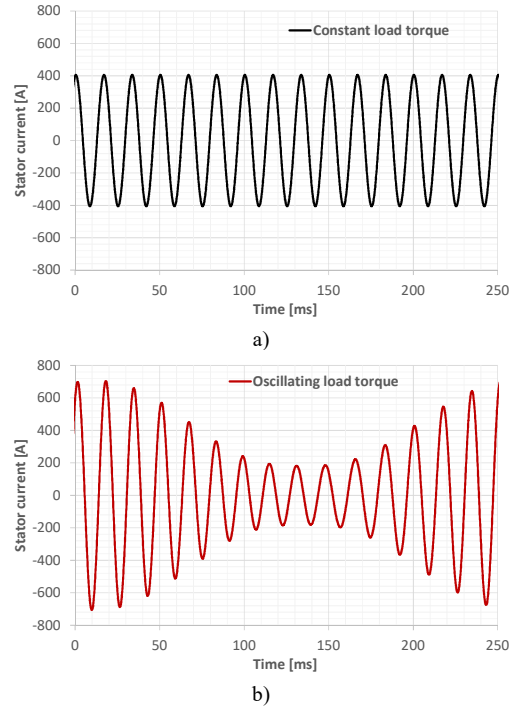


Fig. 12. Waveforms of stator currents simulated for the 6 MW synchronous motor SM3. a) Rated load torque. b) Rated load torque plus an oscillating component of half the rated torque at a frequency of 4 Hz.

The 60 Hz fundamental components of the currents in Figures 12a and 12b are roughly equal. The current in Figure 12b has the oscillation harmonics at frequencies 56 Hz and 64 Hz. Their amplitudes are 46% and 45% of the fundamental harmonic, respectively.

As the core losses are not much affected, simpler models, such as the two-axis model or space-vector model could have been used for the loss analysis. A double- or triple-cage model would have been needed for the skin effect of the rotor cage [17]. The dependence of the additional losses on the vibration amplitude and frequency could have been extracted with good accuracy using one of these relatively simple circuit models.

The results show clearly the importance of torsional drive-train design of reciprocating compressors. The magnetic damping of the rigid-body mode is large. A drive-train designer may use this for vibration control but it has to be kept in mind that the large damping is closely related to large additional loss. At the rigid-body resonance, this may lead to unacceptably large temperature rise particularly on the rotor side of the machine. From drive-train design point of view it is important to avoid the resonance of the rigid-body mode.

It is significant that both the mechanical and electrical criteria set in the standards are needed to limit the vibrations of these systems. Even if the criteria are fulfilled, the additional losses may grow large and lead to premature failure

of the insulation system of a motor.

In general, it is difficult to detect torsional vibration of rotating machinery. For electrical machines, the harmonic stator currents induced at frequencies  $f_s \pm f_v$  should be relatively good vibration indicators. If the amplitudes of these currents grow to, say 20% of the rated current, one should become concerned of the thermal status of the machine.

## V. CONCLUSION

An electrical machine in a drive train allows a rigid-body vibration mode at non-zero frequency. The amplitude of this mode may grow large enough to induce significant additional losses in the electrical machine. Standards indirectly limit the vibration amplitude and losses of the machine by putting constraints on the torque in shaft coupling and on harmonic contents of the line current.

The losses were studied using time-discretized finite element analysis for six induction motors and six synchronous machines. The constraint on the coupling torque effectively restricts the losses at higher frequencies, the constraint on the harmonic current is effective close to the rigid-body resonance frequency. Taking these constraints into account, the maximum increase of electromagnetic loss within the six studied induction motors was about 20% and within the six synchronous machines 75%. Such an additional loss would significantly increase the temperature rise of the machine and reduce its load capacity.

Comparison of the measured and computed results shows that the method used for the loss analysis is valid for this kind of a torsional vibration study.

## REFERENCES

- [1] E. F. Merrill, "Torsional dynamics of AC electrical machines and systems". Proceedings of IEEE Pulp and Paper Industry Conference. pp 52-59, 1994.
- [2] C. Concordia, "Induction motor damping and synchronizing torques". AIEE Trans. Power Apparatus and Systems, vol. 71, pp. 364-366, 1952.
- [3] J. Song-Manguelle; C. Sihler; S. Schramm, "A general approach of damping torsional resonance modes in multimewatt applications". IEEE Transactions on Industry Applications, Vol. 47, Iss. 3, pp. 1390-1399, 2011.
- [4] G. Knop, "The importance of motor dynamics in reciprocating compressor drives". Proc. 8th Conf. EFRC, Sep 27-28 2012, Düsseldorf, Germany.
- [5] E. Hauptmann, B. Howes, B. Eckert, "The influence on torsional vibration analysis of electromagnetic effects across an induction motor air gap". Proc. of Gas Machinery Research Council, Albuquerque, New Mexico, 2013.
- [6] J. S. Joyce; T. Kulig; D. Lambrecht, "Torsional fatigue of turbine-generator shafts caused by different electrical system faults and switching operations". IEEE Transactions on Power Apparatus and Systems, Vol. 97, Iss. 5, pp. 1965-1977, 1978
- [7] I. M. Canay, H. J. Rohrer; K. E. Schnirel; "Effect of electrical disturbances, grid recovery voltage and generator inertia on maximization of mechanical torques in large turbogenerator sets". IEEE Transactions on Power Apparatus and Systems, Vol 99, Iss. 4, pp, 1357-1370, 1980.
- [8] C. E. J. Bowler, "Grid induced torsional vibrations in turbine-generators — Instrumentation, monitoring, and protection". IEEE Power and Energy Society General Meeting, pp. 1-7, 2012.
- [9] J. Licari, C. E. Ugalde-Loo, J. B. Ekanayake, N. Jenkins, "Damping of torsional vibrations in a variable-speed wind turbine". IEEE Transactions on Energy Conversion, Vol. 28, Iss. 1, pp. 172-180, 2013.
- [10] API Standard 671: Special Purpose Couplings for Petroleum, Chemical and Gas Industry Services, Fourth Edition, August 2007. Identical to ISO 10441:2007. Sections 6.6 – 6.7.
- [11] ANSI/API Standard 618-2008: Reciprocating Compressors for Petroleum, Chemical, and Gas Industry Services. Fifth edition, December 2007, Section 7.1.2.6.
- [12] A. Arkkio, "Finite element analysis of cage induction motors fed by static frequency converters". IEEE Trans. Magnetics, 26(2), pp. 551-554, 1990.

- [13] B. Davat, Z. Ren, M. Lajoie-Mazenc, "The movement in field modeling," IEEE Trans. Magnetics, 21 (6), pp. 2296-2298, 1985.
- [14] J. L. Coulomb, "A methodology for the determination of global electromechanical quantities from a finite element analysis and its application to the evaluation of magnetic forces, torques and stiffness," IEEE Trans. Magnetics, 19 (6), p. 2514-2519, 1983.
- [15] A. M. Knight, J. C. Salmon, J. Ewanchuk, "Integration of a first order eddy current approximation with 2D FEA for prediction of PWM harmonic losses in electrical machines". IEEE Trans. Magnetics 49 (5), pp. 1957–1960, 2013.
- [16] A. Arkkio, A. Niemenmaa, "Estimation of losses in cage induction motors using finite element techniques". International Conference on Electrical Machines, 15–17 September 1992, Manchester, UK. Vol. 2, pp. 317–321.
- [17] A. Arkkio, T. P. Holopainen, "Space-vector models for torsional vibration of cage induction motors". IEEE Trans. Ind. Applications, 52 (4), pp. 2988–2995, 2016.
- [18] A. Arkkio, J. Westerlund, "An electromechanical model for analysing transients in diesel-driven synchronous generators". International Conference on Electrical Machines, 28–30 August 2000, Espoo, Finland. Vol. 2, pp. 878–882.



**Antero Arkkio** received his M.Sc. (Tech.) and D.Sc. (Tech.) degrees from Helsinki University of Technology in 1980 and 1988. Currently he is a Professor of Electrical Engineering at Aalto University. His research interests deal with modeling, design, and

measurement of electrical machines.



**Samuli Cederström** started his studies at Aalto University School of Electrical Engineering, Espoo, Finland, in 2014. He is currently working as a research assistant in the Research Group of Electromechanics while studying towards his B.Sc. degree.



**Hafiz Asad Ali Awan** received the B.Sc. degree in electrical engineering from the University of Engineering and Technology, Lahore, Pakistan, in 2012 and the M.Sc. (Tech.) degree in electrical engineering from Aalto University, Espoo, Finland, in 2015. He is currently working toward the

D.Sc. (Tech.) degree at Aalto University. His main research interest is the control of electric drives.



**Seppo E. Saarakkala** received the M.Sc. (Eng.) degree from the Lappeenranta University of Technology, Lappeenranta, Finland, in 2008, and the D.Sc. (Tech.) degree in electrical engineering from Aalto University, Espoo, Finland, in 2014. He has been with the School of Electrical Engineering, Aalto University, since 2010,

where he is currently a Post-Doctoral Research Scientist. His main research interests include control systems and electric drives.



**Timo P. Holopainen** received his M.Sc. degree in 1987 from Helsinki University of Technology, Mechanical Engineering. He began his career at VTT Manufacturing Technology working with strength and vibration control of marine structures. Later, he focused on vibrations of rotating machines and received his D.Sc. (Tech.)

degree from Helsinki University of Technology, Electrical Engineering. Currently he works with rotordynamics and vibration control of large electric motors at ABB Motors and Generators, Technology Development. He is a member of API 684 Task Force (Rotordynamic Tutorial) and IFToMM Technical Committee for Rotordynamics.